Published in final edited form as:
Brain Res. 2007 July 16; 1158: 103–115. doi:10.1016/j.brainres.2007.04.070.

Strain rate-dependent induction of reactive astrogliosis and cell death in three-dimensional neuronal-astrocytic co-cultures

Daniel Kacy Cullen, Ph.D.,
Coulter Department of Biomedical Engineering Georgia Institute of Technology/Emory University, 313 Ferst Dr., Atlanta, GA 30332-0535 Ph: 404-385-5051 Fx: 404-385-5044
dkacy@neuro.gatech.edu

Crystal Michelle Simon, B.S.E., and
Coulter Department of Biomedical Engineering Georgia Institute of Technology/Emory University, 313 Ferst Dr., Atlanta, GA 30332-0535 Ph: 404-385-5051 Fx: 404-385-5044
crystal.simon@bme.gatech.edu

Michelle Camille LaPlaca, Ph.D.
Coulter Department of Biomedical Engineering Georgia Institute of Technology/Emory University, 313 Ferst Dr., Atlanta, GA 30332-0535 Ph: 404-385-0629 Fx: 404-385-5044
michelle.laplaca@bme.gatech.edu

Abstract

A mechanical insult to the brain drastically alters the microenvironment as specific cell types become reactive in an effort to sequester severely damaged tissue. Although injury-induced astrogliosis has been investigated, the relationship between well-defined biomechanical inputs and acute astrogliotic alterations are not well understood. We evaluated the effects of strain rate on cell death and astrogliosis using a three-dimensional (3-D) *in vitro* model of neurons and astrocytes within a bioactive matrix. At 21 days post-plating, co-cultures were deformed to 0.50 shear strain at strain rates of 1, 10, or 30 s^{-1}. We found that cell death and astrogliotic profiles varied differentially based on strain rate at two days post-insult. Significant cell death was observed after moderate (10 s^{-1}) and high (30 s^{-1}) rate deformation, but not after quasi-static (1 s^{-1}) loading. The vast majority of cell death occurred in neurons, suggesting these cells are more susceptible to high rate shear strains than astrocytes for the insult parameters used here. Injury-induced astrogliosis was compared to co-cultures treated with transforming growth factor β, which induced robust astrocyte hypertrophy and increased glial fibrillary acidic protein (GFAP) and chondroitin-sulfate proteoglycans (CSPGs). Quasi-static loading resulted in increased cell density and CSPG secretion. Moderate rate deformation increased cell density, GFAP reactivity, and hypertrophic process density. High rate deformation resulted in increased GFAP reactivity; however, other astrogliotic alterations were not observed at this time-point. These results demonstrate that the mode and degree of astrogliosis depend on rate of deformation, demonstrating astrogliotic augmentation at sub-lethal injury levels as well as levels inducing cell death.

Corresponding author: Michelle Camille LaPlaca, Ph.D. GT/Emory Coulter Department of Biomedical Engineering 313 Ferst Dr. Atlanta, GA 30332-0535 Ph: 404-385-0629 Fx: 404-385-5044 michelle.laplaca@bme.gatech.edu.

Keywords

astrogliosis; shear strain; cell biomechanics; in vitro; mechanotransduction; TBI

1. Introduction

Traumatic brain injury (TBI) initiates complex physical and biochemical alterations that drastically alter the microenvironment, ultimately limiting regenerative capabilities. A perturbation to neural homeostasis may induce a potent reactive response resulting in the formation of the glial scar, a physical and chemical barrier formed in an attempt to isolate injured tissue from the penumbra. The post-insult reactive response involves the recruitment/activation of many cell types including astrocytes, macrophages, microglia, oligodendrocytes, and meningeal cells, ultimately coalescing into the glial scar (Fawcett and Asher, 1999; McGraw et al., 2001). The formation of a glial scar appears to have short-term positive effects following neurotrauma as it may decrease the extent of tissue damage through localization of the inflammatory response and re-establishment of the blood-brain barrier (Bush et al., 1999). However, the chronic glial scar, consisting primarily of a tightly interwoven meshwork of hypertrophic astrocytes and their processes, ultimately hinders regeneration as it contains specific extracellular matrix (ECM) components that have been shown to be inhibitory to neurite outgrowth (McKeon et al., 1995; McKeon et al., 1999; Asher et al., 2000). Reactive astrogliosis is one of the major hallmarks of the glial scar and involves increased expression of intermediate filaments (e.g., glial fibrillary acidic protein (GFAP)), hypertrophy, hyperplasia, and increased matrix production/secretion (e.g., chondroitin sulfate proteoglycans (CSPGs) and laminin) (Fawcett and Asher, 1999; Morgenstern et al., 2002). Several signaling molecules that induce or amplify the astrogliotic response have been identified, such as cytokines (e.g., fibroblast growth factor (FGF) (Li et al., 1997); transforming growth factor beta (TGF-β) (Logan et al., 1994; Moon and Fawcett, 2001)) and/or nucleotides (e.g., adenosine triphosphate (ATP) (Neary et al., 2003; Neary et al., 2006)), however, an improved understanding of the complex mechanisms underlying the induction of reactive astrogliosis and chronic glial scarring may eventually lead to strategies for of repair and regeneration.

The reactive astrogliotic environment and chronic glial scar have been extensively characterized using a range of systems. *In vivo* studies of brain and spinal cord injury have characterized the time-course and degree of inflammation and reactive astrogliosis, providing insight into the physiology of reactive astrocytes and associated matrix alterations (Mathewson and Berry, 1985; Janeczko, 1989; Cervos-Navarro and Lafuente, 1991; Fitch et al., 1999; McKeon et al., 1999; Goussev et al., 2003; Moon et al., 2004). Such *in vivo* models aid in characterizing the complex reactive astrogliotic response; however, the distinction between causative factors and epiphenomena surrounding the isolation of induction mechanisms remains challenging. *In vitro* models offer a high degree of experimental control, providing the ability to impart defined mechanical inputs and assess the resulting cellular alterations. Direct strain transfer to astrocytes may be an initiating factor for astrogliotic alterations via mechanosensation or mechanotransduction, the process by which cells convert mechanical stimuli into changes in intracellular biochemical signaling (Guharay and Sachs, 1984; Bowman et al., 1992; Ingber, 1997; Alenghat and Ingber, 2002; Kamm and Kaazempur-Mofrad, 2004). Mechanosensitive elements may directly affect ion homeostasis in astrocytes. For instance, direct strain to astrocytes has been shown to increase cytosolic calcium from both extracellular and intracellular sources, which increased with more severe insults; however, these experiments did not independently isolate the effects of strain and strain rate (Rzigalinski et al., 1998; Floyd et al., 2001; Neary et al., 2003). Additionally, mechanical stress may open stretch-activated ion channels,

leading to increased intracellular calcium (Bowman et al., 1992; Rzigalinski et al., 1998; Floyd et al., 2005). Thus, astrocytes may possess mechanisms to directly respond to mechanical stress and the associated deformation in both physiological and pathophysiological settings. There is likely a continuum of astrocytic responses to mechanical perturbation ranging from transient reactivity to cell death; therefore, there is a critical need to elucidate tolerances to traumatic loading in order to develop mechanistically-driven intervention strategies.

Although previous studies in both *in vitro* and *in vivo* models have reported a robust astrogliotic response proportional to injury severity, the relationships between biomechanical inputs and the resulting astrocytic responses are not well-defined. Accordingly, we hypothesized that strain rate influences cellular responses following mechanical injury, resulting in varying degrees of cell death and astrogliotic alterations. To test this hypothesis, we utilized a well-characterized *in vitro* injury model in which shear deformation was imparted to thick (>500 μm) three-dimensional (3-D) neuronal-astrocytic co-cultures at a prescribed strain rate and magnitude (LaPlaca et al., 2005; Cullen and LaPlaca, 2006). This *in vitro* injury model reduces some of the complexity associated with *in vivo* experiments, thus minimizing potentially confounding variables and facilitating more direct investigation of the effects of mechanical insult severity. This *in vitro* system models key elements of mechanical trauma *in vivo* due to the 3-D architecture of the system, appropriate to generate complex, heterogeneous biomechanics (Cullen and LaPlaca, 2006) and the multi-cellular composition (i.e., neuronal and astrocytic). After subjecting 3-D co-cultures to mechanical deformation at various strain rates, we evaluated cell viability, cell density, astrogliotic parameters (e.g., hypertrophy, GFAP expression), and ECM alterations (e.g., CSPG expression). Our findings demonstrate that the level of cell death as well as the mode and degree of astrogliosis depend significantly on strain rate, thus implicating this biomechanical parameter in astrocytic mechanotransduction.

2. Results

2.1 Cell Viability Following Mechanical Loading or TGF-β1 Treatment

At 21 days *in vitro* (DIV) 3-D neuronal-astrocytic co-cultures were subjected to static control conditions, TGF-β1 treatment, or subjected to variable rate shear deformation using the 3-D cell shearing device (CSD) (Fig. 1). Two days following deformation, viability, total cell density, and dead cell density were each found to depend significantly on strain rate ($p < 0.05$) (Fig. 2). Specifically, the highest rate deformation (30 s^{-1}) resulted in a significant reduction in culture viability ($p < 0.05$). However, there was not a statistically significant change in the percentage of viable cells from either the quasi-static deformation (1 s^{-1}) or the moderate rate deformation regime (10 s^{-1}) compared to controls (Fig. 2F). TGF-β1 treatment had no effect on culture viability compared to controls. Although there was an increasing trend in overall cell density in all groups versus controls, these increases were only statistically significant for the quasi-static ($p < 0.001$) and moderate rate ($p < 0.01$) deformation regimes (Fig. 2G), suggesting a proliferative response initiated by mechanical deformation over a range of loading rates. Due to this increase in cell density, it was possible that detrimental effects on culture viability due to the mechanical insult were masked when calculating the percentage of viable cells. Accordingly, the density of dead cells was analyzed, revealing that there was a significant increase in the dead cell density following both moderate and high rate deformation ($p < 0.05$) (Fig. 2G). These results demonstrate changes in cell death and cell density in a strain rate-dependent manner, as a low strain rate (1 s^{-1}) led to increased cell density, suggesting a hyperplasic response, whereas a high strain rate (30 s^{-1}) resulted in cell death. Moreover, a moderate strain rate (10 s^{-1}) caused cell death in a subpopulation, with a concurrent hyperplasic response.

2.2 Determination of Neuronal versus Astrocytic Cell Death

A TUNEL assay was performed to label DNA strand breaks, indicating cell death, in conjunction with immunocytochemistry (GFAP, astrocyte marker; MAP-2, neuron marker) to identify the phenotype of live and dead cells at two days post-insult. Confocal and two-photon imaging revealed that the majority of $TUNEL^+$ cells were also immunopositive for MAP-2, with a paucity of double-labeling with GFAP. These observations indicate that the majority of cell death was restricted to the neuronal population withing the co-cultures (Fig. 3). Similar results were observed following both moderate and high rate deformation, suggesting that neurons have a lower biomechanical threshold for cell death compared to astrocytes for shear strain insults.

2.3 Establishment of Astrogliotic Markers

Astrocyte reactivity and increases in CSPG expression have been well-documented following *in vivo* injury; however, these responses required validation in our *in vitro* co-culture system. Co-cultures were subjected to longer-term TGF-β1 treatment (from 21 – 36 DIV) as a positive pro-astrogliotic control environment or left as untreated controls. At 36 DIV, co-cultures were immunolabeled for GFAP and CSPGs. This longer-term TGF-β1 treatment induced dramatic alterations in astrocytic process density and hypertrophy compared to untreated controls (Fig. 4A, B). Furthermore, there were stark increases in CSPG accumulation in TGF-β1 treated cultures versus controls (Fig. 4C, D). This established specific outcome measures (astrocytic hypertrophy and CSPG expression) for subsequent experiments and validated the use of TGF-β1 as a positive control for induction of reactive astrogliosis, which is consistent with previous reports (Logan et al., 1994).

2.4 Astrocyte Hypertrophy Following Mechanical Loading or TGF-β1 Treatment

Co-cultures were immunolabeled for GFAP with a nuclear counterstain at two days post-insult to assess the overall density of astrocytic processes and the density of hypertrophic processes. There was increased GFAP reactivity (intensity and process density) following TGF-β1 treatment and mechanical deformation compared to controls (Fig. 5). Both TGF-β1 treatment and moderate rate deformation ($10\ s^{-1}$) induced signicant alterations in the density of hypertrophic processes ($p < 0.05$) (Fig. 5F). The density of cell nuclei also increased following deformation versus controls, corroborating the earlier results obtained using 3-D confocal microscopy ($p < 0.05$). There was a modest increase in the density of hypertrophic processes following quasi-static and high rate loading; however. these changes were not statistically significant. Although, there was a significant increase in the density of hypertrophic processes following high rate deformation versus controls by five days post-insult (data not shown). The severity of high strain rate loading may influence the apparent lag in the increase in hypertrophic process density, thus necessitating recovery time for the process density to increase beyond pre-injury levels.

2.5 CSPG Expression Following Mechanical Loading or TGF-β1 Treatment

Matrix alterations characteristic of reactive astrogliosis were evaluated following mechanical loading or TGF-β1 treatment using a general immunomarker for CSPGs and a quantitative assay to detect CSPGs in the medium surrounding the cell-containing matrices. At two days post-insult, the matrix content of CSPGs increased following TGF-β1 treatment compared to controls ($p < 0.001$) (Fig. 6). Although CSPG deposition was observed adjacent to hypertrophic GFAP processes following mechanical loading (Fig. 6D-F), there was no overall increase in CSPG accumulation for any of the loading regimes at this time-point. In addition, the matrix content of neurocan increased following treatment with TGF-β1, but such alterations were not apparent following mechanical loading (data not shown). When the total CSPG content in the medium was assessed, increases of 53.4% and 83.8% were found

following TGF-β1 treatment and quasi-static deformation, respectively ($p < 0.05$) (Fig. 6H). The CSPG content in the medium remained near baseline levels following moderate and high rate deformation. Thus, quasi-static deformation and TGF-β1 treatment resulted in increased CSPG secretion, whereas moderate and high rate loading did not significantly alter CSPG expression at this time-point.

3. Discussion

The goal of this study was to evaluate neural cell death and reactive astrogliosis as a function of strain rate (for large magnitude shear strain) to better understand tissue responses to mechanical loading associated with TBI. The loading parameters we utilized are consistent with injury thresholds associated with acceleration-deceleration loading, where diffuse strain patterns may have magnitudes of 0.10 – 0.50 at strain rates of 10 – 50 s^{-1} (Margulies and Thibault, 1989; Margulies et al., 1990; Meaney et al., 1995). Specifically, we evaluated cell viability and markers of astrogliosis in mature 3-D neuron-astrocyte co-cultures subjected to a range of mechanical loading regimes (0.50 strain at 1, 10, or 30 s^{-1} strain rate), TGF-β1 treatment (a factor inducing astrogliosis (Logan et al., 1994)) or control conditions, revealing that cell death as well as specific astrogliotic alterations were dependent on strain rate. Co-cultures subjected to quasi-static loading (1 s^{-1}) produced changes that were potentially within a physiological response range, including increased cell density and CSPG secretion with no significant cell death, demonstrating that sub-lethal deformations can induce astrogliotic alterations. The observed increase in cell density at this sub-lethal deformation level was likely due to a hyperplasic astrocytic response initiated within hours of the mechanical insult, as previously described following mechanical injury (Li et al., 1997; Muir et al., 2002; Neary et al., 2006). Moderate rate injury (10 s^{-1}) resulted in increased cell death with a concomitant increase in astrocytic hypertrophy and cell density, suggesting a hypertrophic and hyperplasic response. High rate deformation (30 s^{-1}) decreased cell viability with no increase in cell density or CSPG accumulation, perhaps indicating that this mechanical injury was too severe to induce characteristic astrogliotic alterations by this time-point. Interestingly, cell death following moderate or high rate deformation was predominantly neuronal, indicating that astrocytes may be more resilient to diffuse shear strains than neurons, and thus less likely to initiate pathways leading to cell death. Collectively, these results indicate that neural cells are sensitive to strain rate for the case of large magnitude deformation.

The observed increases in astrocyte reactivity and hypertrophy were consistent with other studies evaluating the astrocytic response to mechanical injury, which demonstrated that a central event of astrogliosis was enhanced GFAP expression with associated hypertrophy (Li et al., 1997; Muir et al., 2002). However, matrix-bound CSPG accumulation following mechanical loading was not observed to the degree of that seen following TGF-β1 treatment, potentially due to differences in the reactive responses based on the mode of induction or insult severity. Taken together, these results suggest that the rate of deformation imparted to neuronal-astrocytic co-cultures at least partially dictates the cellular response, encompassing astrogliotic alterations and cell death, depending on the severity of the loading parameters, as proposed in Fig. 7. Specifically, at relatively low magnitude, low strain rates, such as those that may be experienced under physiological conditions due to typical fluctuations in intracranial pressure or tissue swelling/settling, may produce little or no cellular response. However, as the insult severity increases, high magnitude deformation, not normally experienced by the CNS, induces reactive astrocytotic responses when applied at low rates, whereas moderate strain rates may surpass cellular thresholds and result in significant neuronal cell death with a concurrent astrocytotic reactive response. Moreover, large magnitude, high rate loading parameters induces significant neuronal death, but may be too severe to result in a programmed reactive response in astrocytes.

The strain rates chosen for this study ranged from sub-lethal to severe levels (LaPlaca et al., 2005; Cullen and LaPlaca, 2006). This distinction permitted the assessment of the effects of a direct mechanical insult with and without local cell death on astrogliotic induction in a 3-D environment. It should be noted that strain inputs were based on *bulk* displacement of 3-D cell-containing matrices; however, as we have previously shown, local cellular strain manifestation is complex and heterogeneous as a function of cell orientation within the matrix (Cullen and LaPlaca, 2006). Similarly, our outcome measures were based on cumulative culture alterations, and we cannot rule out cell-specific changes following loading that did not alter aggregate outcome measures. Nonetheless, the relative alterations in cell viability following the loading regimes used in this study are consistent with those following both *in vivo* and *in vitro* models of neural trauma (Gennarelli et al., 1982; Ellis et al., 1995; Meaney et al., 1995; Ahmed et al., 2000). Strain rate-dependent responses to mechanical loading have previously been reported for neural cells (Ellis et al., 1995; Cargill and Thibault, 1996; LaPlaca et al., 1997; Geddes and Cargill, 2001; LaPlaca et al., 2005), but this is the first report of such a response in neural co-cultures based on 3-D biomechanical inputs.

Models consisting of multiple neural cell types grown in 3-D may maintain many positive aspects of *in vitro* modeling while more closely approximating the cellular heterogeneity and cytoarchitecture of the brain. *In vitro* models provide a simplified experimental paradigm that can be used to remove some potentially dominant systemic influences of astrogliotic induction (e.g., compromise of the blood-brain barrier), permitting evaluation and manipulation of specific facets of the reactive response in a controlled setting. Previous models for the *in vitro* investigation of specific astrogliotic induction mechanisms following mechanical trauma have utilized 2-D culture systems, which may fail to fully capture certain physiologically-relevant induction mechanisms, such as ECM-bound factors, elements of autocrine/paracrine signaling, and the influence of other neural cell types. Astrocytes and neurons have an intricate coupling as astrocytes provide physical and metabolic support by providing trophic factors, maintaining balanced energetics/metabolism, guiding neurite outgrowth and regulating the synaptic microenvironment (Ullian et al., 2001; Tsacopoulos, 2002). Following trauma, astrocytes have the potential to rescue and protect neurons by producing and secreting neurotrophic factors and reducing intracellular neuronal calcium currents (McIntosh et al., 1999; Vivien and Ali, 2006). The presence of neurons may also affect astrocytic responses such as neurotrophin production and proliferation (Hatten, 1987; McIntosh et al., 1999). Thus, the *in vitro* model used here provides an intermediate degree of complexity between *in vivo* and 2-D *in vitro* systems by representing neuronal-astrocytic interactions in a 3-D architecture that can be subjected to defined biomechanical inputs. Thus, this co-culture system is well-suited for the investigation of cellular tolerances to mechanical injury, which can be explored based on the overall injury parameters (e.g., strain magnitude and rate), the 3-D local cellular strain manifestation (Cullen and LaPlaca, 2006), and the presence of various neural cell types, an analysis currently not possible with other models of neural trauma. Establishing such tolerances may be beneficial in understanding the pathophysiology of trauma as a function of specific loading parameters, hence leading to more directed therapeutic targets as well as preventative measures.

The strain rate-dependent astrogliotic alterations observed in this study may be explained by a number of mechanisms, including mechanotransduction or biochemical induction pathways. Mechanotransduction may be initiated by any number of mechanisms, including deformation of stretch-activated ion channels or activation of integrin-mediated signaling pathways. In support of this concept, it has previously been noted that the spatiotemporal profile of the astrogliotic response is correlated with the distribution of mechanical stress throughout the brain (Mathewson and Berry, 1985). In addition, the morphology of astrocytes, comprised of numerous long processes arranged in a meshwork throughout the

brain, presents an ideal architecture for the detection of mechanical disturbances (Ostrow and Sachs, 2005). Stretch-activated ion channels in astrocytes become permeable to cations when mechanical force is applied (Bowman et al., 1992). Astrocytic mechanotransduction may also involve integrins, transmembrane proteins linking cells to ECM that, when physically deformed, activate intracellular signaling pathways regulating the activity of enzymes which may result in changes in gene expression to ultimately modify cellular behavior (Roskelley et al., 1994; Sjaastad et al., 1994; Hamill and Martinac, 2001; Ko and McCulloch, 2001; Alenghat and Ingber, 2002; Cavalcanti-Adam et al., 2005). Although the role of integrin-ECM adhesions in mechanotransduction have been well-characterized in other cell types (Katsumi et al., 2004), a link between integrin-mediated astrogliotic alterations and biomechanical inputs has not been established. However, integrins have been shown to play a significant role in astrocyte migration and proliferation (Etienne-Manneville and Hall, 2001; Nishio et al., 2005), suggesting that mechanical stimulation of these receptors may contribute to the astrogliotic response to mechanical injury. Although our results demonstrate a strain rate-dependence in astrogliotic responses, the role of mechanotransduction as it relates to TBI has not been well-studied and will require further investigation.

Biochemical astrogliotic induction pathways may also contribute to the strain rate-dependent responses observed in this study. For instance, necrotic cell death or disruptions in the plasma membrane may result in the release of glutamate and ATP, which have been shown to induce astrogliosis through receptor binding and subsequent initiation of signaling pathways (Franke et al., 1999; Ahmed et al., 2000; Floyd et al., 2001; Neary et al., 2003; Floyd et al., 2004; Neary et al., 2006). Therefore, the strain rate-dependent cell death may partially explain the variable astrocytotic response at the strain rates evaluated. However, astrogliotic changes were observed at low strain rates ($1\ s^{-1}$) which did not produce significant cell death, suggesting that local cell death is not necessary for initiating pathophysiological responses in astrocytes. Activation of extracellular signal-regulated protein kinase (ERK), a key regulator of cellular proliferation and differentiation, has also been reported at acute time-points post insult (Neary et al., 2003). Furthermore, bFGF and ATP have been implicated in astrogliotic induction as autocrine/paracrine signaling molecules following mechanical injury (Li et al., 1997; Neary et al., 2003). Thus, astrogliotic induction mechanisms may involve a combination of primary mechanosensitive modalities (e.g., receptor stimulation and calcium influx) as well as secondary biochemical mechanisms such as autocrine/paracrine signaling involving positive-feedback release of astrogliosis-inducing factors such as bFGF and ATP.

Although initiated through different events, mechanotransduction and biochemical induction may have some similarities, and future work may elucidate potentially convergent or divergent elements of signaling pathways. However, a similar initiating factor may involve local increases in intracellular calcium. Previous studies of 2-D stretch injury in astrocytes have demonstrated transient increases in intracellular calcium from extracellular and intracellular sources (Rzigalinski et al., 1998; Floyd et al., 2001; Neary et al., 2003). Activation of Group I metabotropic glutamate receptors, altered inositol phosphate production and uncoupling of the phospholipase C signaling pathway have been reported as acute events in astrocytic dysfunction following trauma (Floyd et al., 2001; Floyd et al., 2004). Also, increases in intracellular calcium have been linked to mitochondrial dysfunction and ATP release (Ahmed et al., 2000). Thus, the consequences of increased intracellular calcium concentrations are broad, and may cause a range of aberrant down-stream signaling events.

In summary, this study utilized a well-controlled, 3-D *in vitro* model to investigate alterations in cell viability and specific astrogliotic parameters following mechanical

loading. This is the first report indicating that the mode and degree of astrogliotic induction depend on strain rate under conditions of high magnitude strain, demonstrating that neural cells are sensitive to this biomechanical parameter. This model exhibited localized neuronal cell death and markers of astrogliosis, and presents the unique capability to control these responses based on biomechanical input. This system may be further exploited as an *in vitro* test bed to investigate mechanisms of injury-induced biochemical alterations as well as potential therapeutic targets for prevention of widespread cellular dysfunction, death, and neurodegeneration following neural trauma.

4. Experimental Procedures

4.1 Isolation of Primary Cortical Neurons and Cortical Astrocytes

All procedures involving animals were approved by the Institutional Animal Care and Use Committee (IACUC) of the Georgia Institute of Technology. All reagents were purchased from Invitrogen (Carlsbad, CA) unless otherwise noted. Primary cortical neurons (embryonic day 17) and cortical astrocytes (postnatal day one) were harvested from Sasco Sprague-Dawley rats (Charles River, Wilmington, MA). To harvest cortical neurons, timed-pregnant dams were anesthetized using halothane (Halocarbon, River Edge, NJ) and rapidly decapitated. The uterus was removed by Caesarian section and placed in Ca^{2+}- and Mg^{2+}-free Hanks Balanced Salt Solution (HBSS). Each fetus was removed from the amniotic sac, rapidly decapitated, and the brains removed. The cerebral cortices were isolated and the hippocampal formations were removed. To dissociate the tissue, pre-warmed trypsin (0.25%) + 1 mM EDTA was added for 10 minutes at 37°C. The trypsin-EDTA was then removed and DNase I (0.15 mg/mL; Sigma, St. Louis, MO) in HBSS was added. The tissue was triturated with a flame-narrowed Pasteur pipet and then centrifuged at 1000 rpm for 3 minutes after which the supernatant was aspirated and the cells were resuspended in co-culture medium (Neurobasal medium + 2% B-27 + 1% G-5 + 500 μM L-glutamine).

For astrocyte harvest, postnatal pups were anesthetized using halothane and rapidly decapitated. The brains were removed and the cerebral cortices isolated as described above. Upon isolation, cortices were minced and pre-warmed trypsin-EDTA was added and placed in at 37°C for 5 minutes. DNase was added and the tissue was triturated using a flame-narrowed Pasteur pipet. Medium was added (DMEM/F12 + 10% FBS) and the cells were centrifuged (1000 rpm, 3 minutes) after which the supernatant was aspirated. Cells were resuspended in DMEM/F12 + 10% FBS and transferred to T-75 tissue culture flasks. A nearly pure population of type I astrocytes was isolated according to procedures described elsewhere (McCarthy and de Vellis, 1980). Briefly, at various time-points over the first week in culture, the flasks were mechanically agitated to dislodge less adherent cell types. As the cells approached ~90% confluency they were resuspended using trypsin-EDTA, centrifuged, and replated at a density of 300 cells/mm^2. Astrocytes were used between passages 4-12 for the generation of 3-D cultures to permit phenotypic maturation.

4.2 3-D Primary Cortical Neuronal / Secondary Cortical Astrocytic Co-Cultures

Co-cultures were plated using neurons and astrocytes that were separately isolated and dissociated (as described above) in custom-made cell culture chambers consisting of a glass coverslip below a circular silicone-based elastomer mold (Sylgard 184 and 186, Dow Corning; Midland, MI; cross-sectional area = 2 cm^2). Prior to plating, the chambers were pre-treated with 0.05 mg/mL poly-L-lysine (PLL, Sigma) followed by Matrigel (0.5 mL/well at 0.6 mg/mL, Becton Dickinson Biosciences; Bedford, MA) in Neurobasal medium (each treatment was >4 hours). Co-cultures were plated within Matrigel matrix, which exhibits fluid-like behavior at 4°C to permit homogeneous dispersion of dissociated cells throughout matrix material (2,500 cells/mm^3, 1:1 neuron:astrocyte ratio, final Matrigel

concentration 7.5 mg/mL, 500-750 μm thickness). Cultures were subsequently incubated at 37°C to permit matrix gelation and 3-D cell entrapment (Kleinman et al., 1986), after which 0.5 mL of co-culture medium was added to each well. Cultures were maintained at 37°C and 5% CO_2-95% humidified air, and medium was exchanged at 24 hours post-plating and every two days thereafter. This co-culture system has previously been characterized, demonstrating high viability (approx. 95%) at 21 DIV. Also by 21 DIV, the percentage of neurons relative to the total cell population in co-culture had reduced to approximately 10%, possibly a function of astrocyte proliferation or an indication of neuronal death during culture development (unpublished observations).

4.3 Mechanical Loading Using the 3-D Cell Shearing Device

Neuronal-astrocytic co-cultures were mechanically loaded using the 3-D CSD, a custom-built electromechanical device capable of reproducibly imparting high strain rate shear deformation to 3-D cell-containing matrices (LaPlaca et al., 2005). At the time of injury, cultures were removed from the incubator and mounted within the 3-D CSD. The mechanical action of the device was driven by a linear-actuator (BEI Kimco; San Marcos, CA) coupled to a custom-fabricated digital proportional-integral-derivative controller (25 kHz sampling rate, 16 bit sampling resolution) with closed-loop motion control feedback from an optical position sensor (RGH-34, 400 nm resolution; Renishaw, New Mills, United Kingdom). A trapezoidal input was generated by code written in LabVIEW® (National Instruments; Austin, TX). Lateral motion of the cell chamber top plate with respect to the fixed base of the cell chamber imparts simple shear deformation to the elastically-contained 3-D cell-containing matrices (Fig. 1). At 21 DIV, 3-D co-cultures were deformed to a strain magnitude of 0.50 at strain rates of 1, 10, or 30 s^{-1} or left as control cultures (uninjured/static control). After mechanical deformation, warm medium was added and the cultures were returned to the incubator.

4.4 Cytokine Treatment

Beginning at 21 DIV, a subset of co-cultures were treated with transforming growth factor beta 1 (TGF-β1, 10 ng/mL) diluted in co-culture medium. These cultures were designed to serve as a positive reactivity control as this cytokine has previously been found to induce specific alterations consistent with astrogliosis (Logan et al., 1994).

4.5 Cell Viability

Cell viability was assessed using fluorescent probes for distinguishing live and dead cells. Cell cultures were incubated with ethidium homodimer-1 (4 μM) and calcein AM (2 μM) (Molecular Probes, Eugene, OR) at 37° C for 30 minutes and then rinsed with 0.1 M Dulbecco's Phosphate-Buffered Saline. At 23 DIV (two days following experimental treatment), co-culture viability was assessed following control conditions, TGF-β1 treatment, and mechanical loading at 1, 10 and 30 s^{-1} (n = 5 – 7 per group). Cultures were viewed on a confocal laser scanning microscope (LSM 510, Zeiss, Oberkochen, Germany) and z-stacks were analyzed using LSM Image Browser (Zeiss). The number of viable cells (fluorescing green by AM-cleavage) and the number of cells with compromised membranes (nuclei fluorescing red by ethidium homodimer-1) were quantified (3 – 5 randomly selected regions per culture).

4.6 Markers of Astrogliosis and Determination of TUNEL$^+$ Cell Types

Astrogliotic induction was evaluated two days following mechanical loading (0.50 strain) at strain rates of 1, 10, or 30 s^{-1} in comparison to static control and TGF-β1 treatment co-cultures.

4.6.1 Immunocytochemistry and TUNEL staining—Fluorescent staining was used to assess astrogliotic alterations (e.g., astrocyte hypertrophy/reactivity and matrix alterations) as well as the phenotype of dead or dying cells ($TUNEL^+$). Briefly, 3-D neuronal-astrocytic co-cultures were fixed with 3.7% formaldehyde (Fisher, Fairlawn, NJ) for 60 minutes and then placed in 30% sucrose (Sigma) overnight at 4°C. Co-cultures were then placed in OCT Embedding Compound (Sakura, Tokyo, Japan), flash frozen in liquid nitrogen, sectioned on a cryostat (20 μm thick), and mounted on glass slides. Sections were rinsed in PBS and permeabilized using 0.1% Triton X100 (Kodak, Rochester, NY) + 8% goat serum for 60 minutes. Fluorescent TUNEL staining was performed in a subset of sections using a commercially available kit (TMR red *in situ* cell death detection kit; Roche Applied Science, Indianapolis, IN). Briefly, sections were incubated at 37°C for 1.5 hours in a solution consisting of a 1:100 ratio of terminal transferase and TMR-dUTP, thus binding a fluorescent probe to free 3′ OH ends of DNA. Primary antibodies were added (in PBS + 0.1% Triton X100 + 2% serum) overnight at 4 °C in a humidified chamber. After rinsing, the appropriate secondary fluorophore-conjugated antibodies (FITC or TRITC-conjugated IgG, Jackson Immuno Research or Alexa 488, 546, or 633-conjugated IgG or IgM, Molecular Probes) were added (in PBS + 2% serum) for two hours at 18-24 °C in a humidified chamber. Sections were immunostained using primary antibodies recognizing glial fibrillary acidic protein (GFAP) (AB5804, 1:400; MAB360, 1:400, Chemicon), an intermediate filament expressed by astrocytes (Debus et al., 1983), MAP-2 (AB5622, 1:1000, Chemicon), a microtubule-associated protein expressed by neurons, and CS-56 (C8035, 1:100, Sigma), a general CSPG marker. (n = 3 – 6 per group per marker; each sample stained in triplicate). Counterstaining was performed using Hoechst 33258 (1:1000, Molecular Probes). To control for non-specific antibody binding, control sections were stained only with secondary (fluorescent) antibodies to establish specificity of acquired fluorescence in experimental samples. Co-localization of TUNEL with neurons and/or astrocytes was assessed using two-photon microscopy (Zeiss NSM/NLO 510 confocal/ multi-photon). Astrogliotic alterations were assessed using epifluorescence microscopy (Eclipse TE300, Nikon, Melville, NY) with images digitally captured (DKC5T5/DMC, Sony, Tokyo, Japan) and analyzed using Image-Pro Plus (Media Cybernetics, Silver Spring, MD). The number of $GFAP^+$ hypertrophic processes was quantified per sample area, and matrix CSPG expression was quantitatively assessed based on intensity relative to background using Image-Pro Plus.

4.6.2 CSPG Secretion—Two days following experimental treatment, medium was sampled for analysis from co-cultures treated with TGF-β1, subjected to mechanical loading at 1, 10 and 30 s^{-1}, or controls (n = 3 – 9 per group). CSPG production and extracellular expression in 3-D cultures was quantified using a colorimetric assay (Blyscan®; Biocolor Assays, Newtownabbey, Northern Ireland). Briefly, medium was sampled from the 3-D cultures and treated with 1,9-dimethylmethelyne blue, a specific label for the sulfated polysaccharide component of proteoglycans and/or the protein-free sulfated glycosaminoglycan chains. Colorimetric alterations were assessed using a plate reader and results quantified using a standard curve for CSPG.

4.6.3 Development of Outcome Measures—Co-cultures were subjected to longer-term TGF-β1 treatment and immunostained for markers of reactive astrogliosis in order to determine acceptable outcome measures for this system. Specifically, 3-D neuronal co-cultures were treated with TGF-β1 from 21 – 36 DIV (10 ng/mL, added fresh every other day) or left as untreated controls (n = 4 each). At 36 DIV, cultures were fixed, processed and immunolabeled for GFAP and CS-56 with Hoechst counterstaining (as described above).

4.7 Statistical Analysis

Analysis of variance (ANOVA) was performed on quantitative results from the viability, immunocytochemistry, and colorimetric studies. When significant differences existed between groups, post hoc Tukey's pair-wise comparisons were performed ($p < 0.05$ required for significance in all statistical tests). Data are presented as mean ± standard deviation.

Acknowledgments

Funding for this work was partially provided by NSF (CAREER Award BES-0093830), NIH/NIBIB (EB001014), NSF (EEC-9731643), and the Southern Consortium for Injury Biomechanics at the University of Alabama Birmingham-Injury Control Research Center, through a grant from the National Center for Injury Prevention and Control, Centers for Disease Control and Prevention, Award R49/CE000191 and Cooperative Agreement TNH22-01-H-07551 with the National Highway Traffic Safety Administration. The authors acknowledge Richard Tan and Maggie Wolfson for technical assistance.

Glossary

3-D	three dimensional
ATP	adenosine triphosphate
CNS	central nervous system
CSD	cell shearing device
CSPG	chondroitin sulfate proteoglycan
ECM	extracellular matrix
DIV	days *in vitro*
FGF	fibroblast growth factor
GFAP	glial fibrillary acidic protein
TBI	traumatic brain injury
TGF-β	transforming growth factor β

REFERENCES

Ahmed SM, Rzigalinski BA, Willoughby KA, Sitterding HA, Ellis EF. Stretch-induced injury alters mitochondrial membrane potential and cellular ATP in cultured astrocytes and neurons. J Neurochem. 2000; 74:1951–1960. [PubMed: 10800938]

Alenghat FJ, Ingber DE. Mechanotransduction: all signals point to cytoskeleton, matrix, and integrins. Sci STKE. 2002; 2002:PE6. [PubMed: 11842240]

Asher RA, Morgenstern DA, Fidler PS, Adcock KH, Oohira A, Braistead JE, Levine JM, Margolis RU, Rogers JH, Fawcett JW. Neurocan is upregulated in injured brain and in cytokine-treated astrocytes. J Neurosci. 2000; 20:2427–2438. [PubMed: 10729323]

Bowman CL, Ding JP, Sachs F, Sokabe M. Mechanotransducing ion channels in astrocytes. Brain Res. 1992; 584:272–286. [PubMed: 1381266]

Bush TG, Puvanachandra N, Horner CH, Polito A, Ostenfeld T, Svendsen CN, Mucke L, Johnson MH, Sofroniew MV. Leukocyte infiltration, neuronal degeneration, and neurite outgrowth after ablation of scar-forming, reactive astrocytes in adult transgenic mice. Neuron. 1999; 23:297–308. [PubMed: 10399936]

Cargill RS 2nd, Thibault LE. Acute alterations in [Ca2+]i in NG108-15 cells subjected to high strain rate deformation and chemical hypoxia: an in vitro model for neural trauma. J Neurotrauma. 1996; 13:395–407. [PubMed: 8863195]

Cavalcanti-Adam EA, Tomakidi P, Bezler M, Spatz JP. Geometric organization of the extracellular matrix in the control of integrin-mediated adhesion and cell function in osteoblasts. Prog Orthod. 2005; 6:232–237. [PubMed: 16276432]

Cervos-Navarro J, Lafuente JV. Traumatic brain injuries: structural changes. J Neurol Sci. 1991; 103(Suppl):S3–14. [PubMed: 1940963]

Cullen DK, LaPlaca MC. Neuronal response to high rate shear deformation depends on heterogeneity of the local strain field. J Neurotrauma. 2006; 23:1304–1319. [PubMed: 16958583]

Debus E, Weber K, Osborn M. Monoclonal antibodies specific for glial fibrillary acidic (GFA) protein and for each of the neurofilament triplet polypeptides. Differentiation. 1983; 25:193–203. [PubMed: 6198232]

Ellis EF, McKinney JS, Willoughby KA, Liang S, Povlishock JT. A new model for rapid stretch-induced injury of cells in culture: characterization of the model using astrocytes. J Neurotrauma. 1995; 12:325–339. [PubMed: 7473807]

Etienne-Manneville S, Hall A. Integrin-mediated activation of Cdc42 controls cell polarity in migrating astrocytes through PKCzeta. Cell. 2001; 106:489–498. [PubMed: 11525734]

Fawcett JW, Asher RA. The glial scar and central nervous system repair. Brain Res Bull. 1999; 49:377–391. [PubMed: 10483914]

Fitch MT, Doller C, Combs CK, Landreth GE, Silver J. Cellular and molecular mechanisms of glial scarring and progressive cavitation: in vivo and in vitro analysis of inflammation-induced secondary injury after CNS trauma. J Neurosci. 1999; 19:8182–8198. [PubMed: 10493720]

Floyd CL, Gorin FA, Lyeth BG. Mechanical strain injury increases intracellular sodium and reverses Na+/Ca2+ exchange in cortical astrocytes. Glia. 2005; 51:35–46. [PubMed: 15779085]

Floyd CL, Rzigalinski BA, Sitterding HA, Willoughby KA, Ellis EF. Antagonism of group I metabotropic glutamate receptors and PLC attenuates increases in inositol trisphosphate and reduces reactive gliosis in strain-injured astrocytes. J Neurotrauma. 2004; 21:205–216. [PubMed: 15000761]

Floyd CL, Rzigalinski BA, Weber JT, Sitterding HA, Willoughby KA, Ellis EF. Traumatic injury of cultured astrocytes alters inositol (1,4,5)-trisphosphate-mediated signaling. Glia. 2001; 33:12–23. [PubMed: 11169788]

Franke H, Krugel U, Illes P. P2 receptor-mediated proliferative effects on astrocytes in vivo. Glia. 1999; 28:190–200. [PubMed: 10559778]

Geddes DM, Cargill RS 2nd. An in vitro model of neural trauma: device characterization and calcium response to mechanical stretch. J Biomech Eng. 2001; 123:247–255. [PubMed: 11476368]

Gennarelli TA, Thibault LE, Adams JH, Graham DI, Thompson CJ, Marcincin RP. Diffuse axonal injury and traumatic coma in the primate. Ann Neurol. 1982; 12:564–574. [PubMed: 7159060]

Goussev S, Hsu JY, Lin Y, Tjoa T, Maida N, Werb Z, Noble-Haeusslein LJ. Differential temporal expression of matrix metalloproteinases after spinal cord injury: relationship to revascularization and wound healing. J Neurosurg. 2003; 99:188–197. [PubMed: 12956462]

Guharay F, Sachs F. Stretch-activated single ion channel currents in tissue-cultured embryonic chick skeletal muscle. J Physiol. 1984; 352:685–701. [PubMed: 6086918]

Hamill OP, Martinac B. Molecular basis of mechanotransduction in living cells. Physiol Rev. 2001; 81:685–740. [PubMed: 11274342]

Hatten ME. Neuronal inhibition of astroglial cell proliferation is membrane mediated. J Cell Biol. 1987; 104:1353–1360. [PubMed: 3571332]

Ingber DE. Tensegrity: the architectural basis of cellular mechanotransduction. Annu Rev Physiol. 1997; 59:575–599. [PubMed: 9074778]

Janeczko K. Spatiotemporal patterns of the astroglial proliferation in rat brain injured at the postmitotic stage of postnatal development: a combined immunocytochemical and autoradiographic study. Brain Res. 1989; 485:236–243. [PubMed: 2720410]

Kamm RD, Kaazempur-Mofrad MR. On the molecular basis for mechanotransduction. Mech Chem Biosyst. 2004; 1:201–209. [PubMed: 16783933]

Katsumi A, Orr AW, Tzima E, Schwartz MA. Integrins in mechanotransduction. J Biol Chem. 2004; 279:12001–12004. [PubMed: 14960578]

Kleinman HK, McGarvey ML, Hassell JR, Star VL, Cannon FB, Laurie GW, Martin GR. Basement membrane complexes with biological activity. Biochemistry. 1986; 25:312–318. [PubMed: 2937447]

Ko KS, McCulloch CA. Intercellular mechanotransduction: cellular circuits that coordinate tissue responses to mechanical loading. Biochem Biophys Res Commun. 2001; 285:1077–1083. [PubMed: 11478763]

LaPlaca MC, Lee VM, Thibault LE. An in vitro model of traumatic neuronal injury: loading rate-dependent changes in acute cytosolic calcium and lactate dehydrogenase release. J Neurotrauma. 1997; 14:355–368. [PubMed: 9219851]

LaPlaca MC, Cullen DK, McLoughlin JJ, Cargill RS II. High Rate Shear Strain of Three-Dimensional Neural Cell Cultures: A New In Vitro Traumatic Brain Injury Model. J Biomech. 2005; 38:1093–1105. [PubMed: 15797591]

Li L, Ye Z, Zhu J. Astrogliosis and basic fibroblast growth factor. Zhonghua Bing Li Xue Za Zhi. 1997; 26:8–10. [PubMed: 10072841]

Logan A, Berry M, Gonzalez AM, Frautschy SA, Sporn MB, Baird A. Effects of transforming growth factor beta 1 on scar production in the injured central nervous system of the rat. Eur J Neurosci. 1994; 6:355–363. [PubMed: 8019673]

Margulies SS, Thibault LE. An analytical model of traumatic diffuse brain injury. J Biomech Eng. 1989; 111:241–249. [PubMed: 2779190]

Margulies SS, Thibault LE, Gennarelli TA. Physical model simulations of brain injury in the primate. J Biomech. 1990; 23:823–836. [PubMed: 2384494]

Mathewson AJ, Berry M. Observations on the astrocyte response to a cerebral stab wound in adult rats. Brain Res. 1985; 327:61–69. [PubMed: 3986520]

McCarthy KD, de Vellis J. Preparation of separate astroglial and oligodendroglial cell cultures from rat cerebral tissue. J Cell Biol. 1980; 85:890–902. [PubMed: 6248568]

McGraw J, Hiebert GW, Steeves JD. Modulating astrogliosis after neurotrauma. J Neurosci Res. 2001; 63:109–115. [PubMed: 11169620]

McIntosh TK, Juhler M, Raghupathi R, Saatman KE, Smith DH. Secondary brain injury: neurochemical and cellular mediators. Traumatic brain injury. 1999

McKeon RJ, Hoke A, Silver J. Injury-induced proteoglycans inhibit the potential for laminin-mediated axon growth on astrocytic scars. Exp Neurol. 1995; 136:32–43. [PubMed: 7589332]

McKeon RJ, Jurynec MJ, Buck CR. The chondroitin sulfate proteoglycans neurocan and phosphacan are expressed by reactive astrocytes in the chronic CNS glial scar. J Neurosci. 1999; 19:10778–10788. [PubMed: 10594061]

Meaney DF, Smith DH, Shreiber DI, Bain AC, Miller RT, Ross DT, Gennarelli TA. Biomechanical analysis of experimental diffuse axonal injury. J Neurotrauma. 1995; 12:689–694. [PubMed: 8683620]

Moon C, Ahn M, Kim S, Jin JK, Sim KB, Kim HM, Lee MY, Shin T. Temporal patterns of the embryonic intermediate filaments nestin and vimentin expression in the cerebral cortex of adult rats after cryoinjury. Brain Res. 2004; 1028:238–242. [PubMed: 15527750]

Moon LD, Fawcett JW. Reduction in CNS scar formation without concomitant increase in axon regeneration following treatment of adult rat brain with a combination of antibodies to TGFbeta1 and beta2. Eur J Neurosci. 2001; 14:1667–1677. [PubMed: 11860461]

Morgenstern DA, Asher RA, Fawcett JW. Chondroitin sulphate proteoglycans in the CNS injury response. Prog Brain Res. 2002; 137:313–332. [PubMed: 12440375]

Muir JK, Willoughby KA, Ellis EF. A confocal microscopic examination of the effects of strain (stretch) on cultured neurons and astrocytes. J Neurotrauma. 2002; 19:1361.

Neary JT, Kang Y, Willoughby KA, Ellis EF. Activation of extracellular signal-regulated kinase by stretch-induced injury in astrocytes involves extracellular ATP and P2 purinergic receptors. J Neurosci. 2003; 23:2348–2356. [PubMed: 12657694]

Neary JT, Kang Y, Shi YF, Tran MD, Wanner IB. P2 receptor signalling, proliferation of astrocytes, and expression of molecules involved in cell-cell interactions. Novartis Found Symp. 2006; 276:131–143. discussion 143-137, 233-137, 275-181. [PubMed: 16805427]

Nishio T, Kawaguchi S, Yamamoto M, Iseda T, Kawasaki T, Hase T. Tenascin-C regulates proliferation and migration of cultured astrocytes in a scratch wound assay. Neuroscience. 2005; 132:87–102. [PubMed: 15780469]

Ostrow LW, Sachs F. Mechanosensation and endothelin in astrocytes--hypothetical roles in CNS pathophysiology. Brain Res Brain Res Rev. 2005; 48:488–508. [PubMed: 15914254]

Roskelley CD, Desprez PY, Bissell MJ. Extracellular matrix-dependent tissue-specific gene expression in mammary epithelial cells requires both physical and biochemical signal transduction. Proc Natl Acad Sci U S A. 1994; 91:12378–12382. [PubMed: 7528920]

Rzigalinski BA, Weber JT, Willoughby KA, Ellis EF. Intracellular free calcium dynamics in stretch-injured astrocytes. J Neurochem. 1998; 70:2377–2385. [PubMed: 9603202]

Sjaastad MD, Angres B, Lewis RS, Nelson WJ. Feedback regulation of cell-substratum adhesion by integrin-mediated intracellular Ca2+ signaling. Proc Natl Acad Sci U S A. 1994; 91:8214–8218. [PubMed: 8058782]

Tsacopoulos M. Metabolic signaling between neurons and glial cells: a short review. J Physiol Paris. 2002; 96:283–288. [PubMed: 12445907]

Ullian EM, Sapperstein SK, Christopherson KS, Barres BA. Control of synapse number by glia. Science. 2001; 291:657–661. [PubMed: 11158678]

Vivien D, Ali C. Transforming growth factor-beta signalling in brain disorders. Cytokine Growth Factor Rev. 2006; 17:121–128. [PubMed: 16271500]

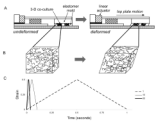

Fig. 1. Schematic of the 3-D neuronal-astrocytic co-culture and mechanical deformation models (not to scale)

Mechanical deformation was imparted to cell-containing matrices through the action of the 3-D Cell Shearing Device (3-D CSD), a custom-built electromechanical device utilizing a linear actuator under closed-loop proportional-integral-derivative control with positional feedback from an optical position sensor (A). Neuronal-astrocytic co-cultures in 3-D were plated throughout the thickness of a bioactive matrix and were laterally constrained by an elastomer mold. Shear deformation of the elastomer mold and cell-embedded matrices was induced through horizontal displacement of the cell chamber top-plate, which was coupled to the linear actuator (B). Input to the system was a symmetrical trapezoidal input to a constant displacement (corresponding to 0.50 bulk shear strain) at strain rates of 1, 10, or 30 s^{-1} (corresponding to rise times of 500, 50, or 16.7 ms, respectively; hold time was held constant at 5 ms) (C).

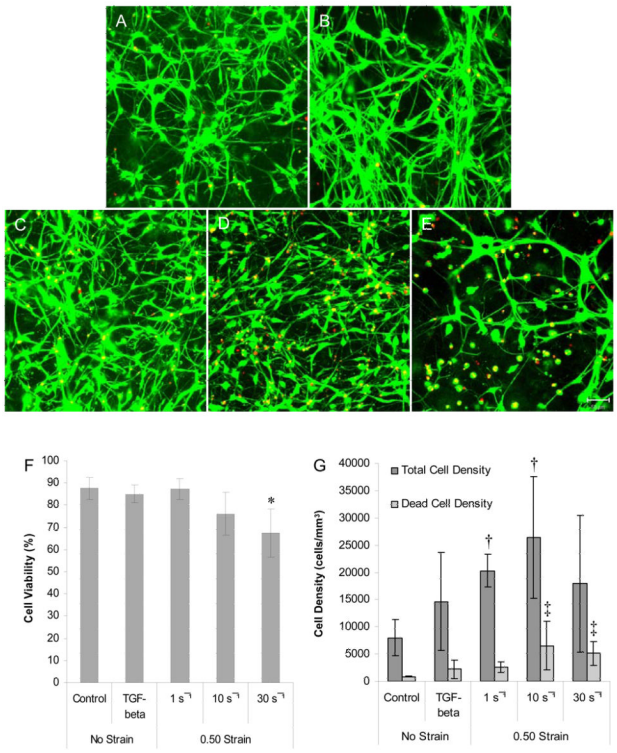

Fig. 2. Culture viability and cell density following mechanical loading or TGF-β1 treatment

3-D neuronal-astrocytic co-cultures were subjected to mechanical deformation, TGF-β1 treatment, or control conditions at 21 DIV and culture viability was assessed two days later. Fluorescent confocal reconstructions of representative co-cultures after control conditions (A), TGF-β1 treatment (B), or mechanical loading at 0.50 strain at low (1 s^{-1}, C), moderate (10 s^{-1}, D), or high (30 s^{-1}, E) strain rates (live cells shown green and nuclei of dead cells shown red; scale bar = 50 μm). High rate deformation resulted in a significant reduction in culture viability* ($p < 0.05$) while quasi-static deformation or TGF-β1 treatment had no effect on culture viability (F). Furthermore, there was a significant increase in cell density following mechanical loading at low and moderate strain rates compared to controls† ($p < 0.05$), suggesting a hyperplasic response. There was also a significant increase in the density of dead cells following moderate and high rate deformation compared to control cultures ‡ ($p < 0.05$).

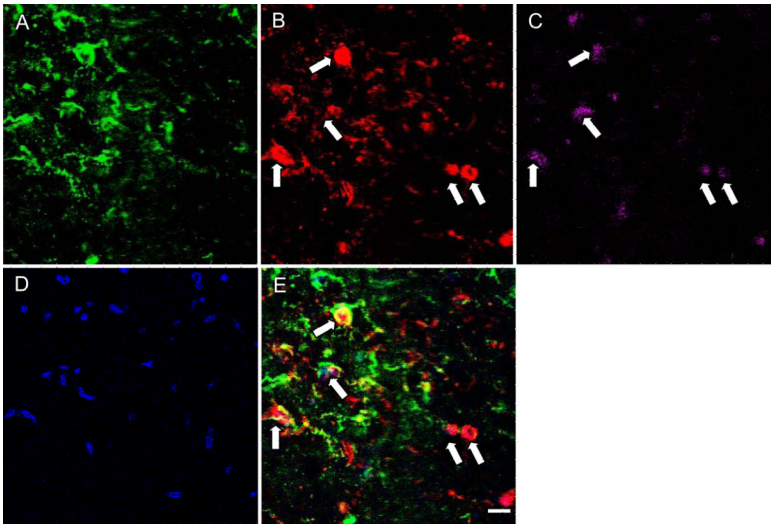

Fig. 3. Assessment of the phenotype of living/dead cells at two days following high strain rate mechanical injury

A fluorescent TUNEL assay was used in conjunction with immunocytochemistry to identify the phenotype of cells undergoing death. GFAP (A) was used to label astrocytes, while MAP-2 (B) was used as a marker for neurons. TUNEL staining labeled the nucleus of dead cells (C), and Hoechst was used as a counterstain for identification of all nuclei within the co-culture (D). TUNEL staining was most prominently found in neurons, with few $TUNEL^{+}$ astrocytes at this time-point. Scale bar = 20 μm.

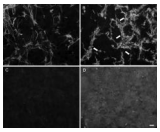

Fig. 4. Derivation of markers of astrogliosis

In order to develop the reactive astrogliotic outcome measures utilized in this study, control co-cultures (A, C) were compared to co-cultures treated with TGF-β1 for 14 days (B, D). Alterations in astrocyte morphology (GFAP) were observed following TGF-β1 (B) as compared to untreated control cultures (A) as many hypertrophic processes were observed (arrows). Also, there were robust increases in CSPG expression in the matrix following 14 day TGF-β1 treatment (D) compared to untreated controls (C). Scale bar = 20 μm.

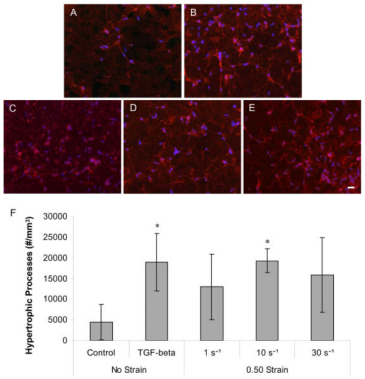

Fig. 5. Astrocyte GFAP reactivity and hypertrophy following mechanical deformation or TGF-β1 treatment

Co-cultures immunolabeled for GFAP (red) with nuclear counterstain (blue) at two days following control (A), TGF-β1 (B), quasi-static (C), moderate rate (D) and high rate (E) deformation (scale bar = 20 μm), revealed increased GFAP reactivity and process density following TGF-β1 treatment and deformation. TGF-β1 treatment and moderate rate deformation induced signicant increases in the density of hypertrophic processes at this time-point compared to control cultures* ($p < 0.05$) (F).

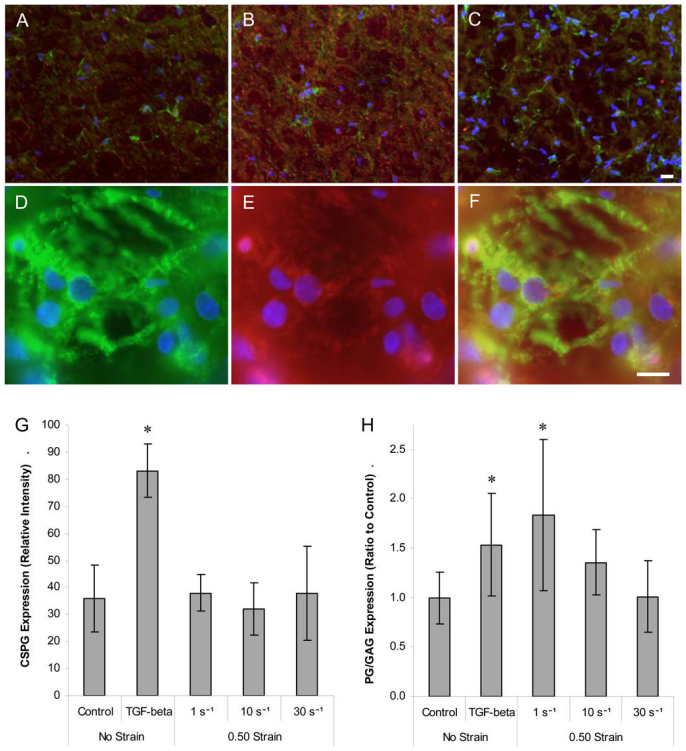

Fig. 6. Expression and localization of CSPGs following deformation or TBF-β1 treatment

Fluorescent micrographs of representative neuronal-astrocytic co-cultures at 23 DIV, two days following control conditions (A), TGF-β1 treatment (B) or high rate deformation (C) (scale bar = 20μm); cultures were immunolabeled for CSPGs (red) and GFAP (green) with nuclear counterstain (blue). $GFAP^{+}$ hypertrophic astrocytes (green) (D) were observed adjacent to CSPGs (red) (E); overlay of previous two photomicrographs (F) following mechanical loading (scale bar = 10μm). There was a significant increase in CSPG deposition in the matrix following TGF-β1* ($p < 0.001$) (G). There were also significant increases in the CSPG content in the medium following quasi-static ($1\ s^{-1}$) deformation and TGF-β1 treatment compared to controls* ($p < 0.05$) PG = proteoglycan; GAG = glycosaminoglycan (H).

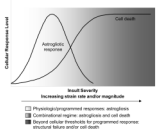

Fig. 7. Postulated astrocytic responses based on mechanical insult severity

Conceptual framework describing a proposed continuum in astrocytic response based on insult severity, ranging from reactive astrogliosis (i.e. programmed physiological response) to necrotic/apoptotic cell death (e.g., surpassing biophysical thresholds).